Motion of a single superconducting vortex

O. B. Hyun, J. R. Clem, and D. K. Finnemore
Ames Laboratory and Department of Physics, Iowa State University, Ames, Iowa 50011
(Received 3 March 1989)

Procedures have been developed to trap a single quantized vortex in a superconducting thin film and systematically move it around under the influence of an applied Lorentz force. The location of the vortex is determined from the diffraction pattern of a Josephson junction formed by superconducting cross strips and a normal-metal barrier; the force is applied by a current in the superconducting film. Vortices move across the junction in a reproducible series of discrete steps, typically a few micrometers long. The elementary pinning force is found to be approximately 10^{-6} N/m in a Pb-Bi film and to vary as $(1-t)^{3/2}$, where t is the reduced temperature. By controlling the pinning sites along a symmetry axis of the junction, one can perform rather simple read and write operations for logic elements.

INTRODUCTION

Procedures recently have been developed to trap a single Abrikosov vortex in a Josephson junction and detect the location of the vortex as it moves from pinning site to pinning site under the influence of an applied force.[1,2] The basic idea is to trap a vortex in a superconducting thin film by field cooling[1] and then detect the location of the vortex by measuring the diffraction pattern of the Josephson junction.[3,4] Distortions in the diffraction pattern from a Fraunhofer pattern give a "signature" which specifies the location of the vortex in the junction. In addition, a force can be applied to the vortex via a transport current, I_p, in one leg of the cross-type junction. This force then pushes the vortex from one pinning site to another at a critical depinning current, I_p^d.

The current, I_p, has two effects in the junction; it applies a force to the vortex in the layer and it causes a magnetic field which can nucleate a new vortex. Close to T_c, the pinning forces are quite small and I_p will move the vortex across the junction without nucleating new vortices. At low temperatures, however, the pinning force for many materials is strong and there is a tendency to nucleate new vortices at the edge of the thin film before the trapped vortex is moved. This arises because there is a self-field associated with I_p which can exceed the critical magnetic field for vortex nucleation before the Lorentz force reaches the critical depinning current, I_p^d. In the preliminary studies, vortex nucleation was the dominant effect observed.[2] For a nucleation process, it is found that the diffraction pattern distorts slightly when the vortex first enters at the edge. One can then follow the vortex as it is pushed into the film.[2] As the temperature increases toward T_c, I_p^d falls more rapidly than I_p^n, and there is a temperature window where vortex pinning can be studied. This window has been studied in some detail for granular Al films,[5] and a preliminary study was made of a Pb-Bi film.[1]

The ability to trap a single vortex in a Josephson junction and to track its motion under the influence of an applied force offers many opportunities for the study of fundamental properties of vortex motion, and it also opens the door for the development of new memory and logic devices based on the motion of a single Abrikosov vortex. For example, using these techniques it is possible to measure the elementary pinning force, f_p, as a function of temperature for various pinning centers and measure the anistropy of the pinning potential.[1] In addition, one can pattern the thin-film superconductor so as to control the location of the pinning centers and thus control the trajectory of the vortex. This could be done, for example, by thinning the film or by overlaying with a normal metal strip. Both would suppress the pair potential in special regions and thus define the path of the vortex.

Two important imaging methods also have been developed in the past few years to detect individual vortices. Both laser beams[6,7] and electron beams in an electron microscope[8,9] have been used, but the detection scheme is rather complicated in that beams of light or electrons must be rastered across the sample. The method used here differs from these in that no external beams are required. It is, in fact, based on the rather different physical principles of diffraction, and one can envisage integrating these latter circuits into arrays of logic devices.

The goal of this work is to study the fundamental processes associated with a motion of a single vortex. Some factors relevant to this motion are the accuracy of locating vortex, the details of the vortex trapping process, the size of the temperature window where depinning can be observed, the self-biasing of a junction using internal currents, the asymmetry of the pinning potential, the reversibility of vortex motion, and the nucleation of new vortices at the edge of the junction. Each of these will be discussed.

EXPERIMENTAL

Many of the experimental details of these measurements have been reported previously,[1-3] so a brief discussion will suffice here. A full discussion is given else-

where,[10] especially the modeling and fitting procedure with inclusion of image vortices to determine the location of the vortex from both the parallel magnetic fields, H_y, and perpendicular field, H_z, diffraction patterns. For the description of the cross-strip Josephson junction used here, axes are chosen with the x axis parallel to the long direction of the top superconducting layer (or secondary layer), the y axis parallel to the bottom superconducting layer (or primary layer) and the z axis perpendicular to the plane of the junction. The axes are placed in the middle of the junction and distances are measured in units of half the junction width, $W/2$, such that x and y coordinates of the junction extend from -1 to 1. Both I_p and the parallel magnetic field to measure diffraction patterns, H_y, are along the y axis. The flux trapping field, H_z^c and perpendicular field for diffraction pattern are along the z axis. For brevity, the superconducting strips are called S layers and the normal metal barrier is called the N layer.

A superconducting thin film 1 cm long, 46 μm wide, and 0.50 μm thick is deposited by flash evaporation of a Pb–2.5 at. % Bi alloy from a resistively heated boat onto a liquid nitrogen cooled glass substrate in a vacuum of 2×10^{-8} TORR. The mask was held approximately 25 μm from the substrate to give a sharp falloff in thickness at the edge. Then an Ag–4 at. % Al normal metal was evaporated by dropping the pellets into a boat one by one immediately after the first Pb-Bi film. Since each pellet contributed about 50 Å thickness, the film should be homogeneous on the scale of the coherence distance of about 300 Å. The second Pb-Bi cross strip was evaporated immediately after the normal metal layer deposition. Delays for moving masks were about 2 min. The same mask rotated through 90° was used for both superconducting strips to assure the square junction assumed in the model.

Data were taken in a ^{3}He cryostat in which temperature was controlled to better than a millikelvin. The current feed for the Josephson current, I_J, was symmetric.[3] Josephson voltages were detected with a rf superconducting quantum interference device (SQUID) to an accuracy of 10^{-12} V. The current leads for the transport current, I_p, had rf filters similar to those used in the SQUID system. Concentric conetic shields were used to reduce the ambient magnetic field to the order of a few millioersted and a superconducting Pb shield was used to screen out stray noise and fields. Superconducting Helmholtz pairs were used to generate magnetic fields perpendicular and parallel to the plane of the junction.

RESULTS AND DISCUSSION

Junction quality

The superconductor–normal-metal–superconductor (SNS) junctions reported here show a free flow of magnetic flux parallel to the junction through the N layer with no irreversibility. The order parameter is so low in this region that there is no effective pinning. Hysteretic behavior occurs only when vortices are trapped in the S layer perpendicular to the film. The junctions showed an excellent Fraunhofer pattern for I_c versus H_y when there were no vortices trapped in the junction. The I_c versus H_z curves showed a good qualitative fit to the theory, but there are the same kind of differences as those reported earlier.[3]

There are two key geometrical factors needed for the success of this experiment. First, the junction must be square, so that the model can be easily used to determine the location of the vortex from the shape of the diffraction patterns. The junctions reported here are, in fact 46-μm square. Second, the N layer must be rather thick to decouple the vortex in the primary S layer from the secondary S layer. If the barrier were very thin, such as in the typical superconductor-insulator-superconductor (SIS) Josephson junction, there would be a strong magnetic coupling of the primary and secondary vortices, such that the vortices would be likely to be aligned, making it difficult to locate the vortices according to the model.[11–16] Also, it would be difficult to isolate a vortex in just one of the films so that the pinning force could be measured. Here the barrier is a 0.8-μm-thick Ag-Al film so that the magnetic coupling force is only a few percent of the pinning force.

In the initial stages of the experiment, the junction was cooled below the transition temperature, T_c, and the current-voltage curves were measured. Resistively shunted junction behavior is approximately followed with $V=R_n(I_J^2-I_c^2)^{1/2}$ for $I_J>I_C$ and $V=0$ for $I_J<I_c$. The value of the barrier resistance, R_n, increases as T approaches T_c because of quasiparticle relaxation effects as reported by Hsiang and Clarke.[17] Values of R_n derived from I-V curves are typically $\frac{3}{4}$ of the values of R_n derived from separate Ag strips deposited at the same time as the barrier. Since the current flows perpendicular to the film in one case and parallel in the other, this is rather good agreement. As the temperature approaches T_c there also is some rounding of I-V curve close to the $V=0$ point. This rounding resulted in about 3% uncertainly in I_c at 7.0 K. The value of I_c was defined by extrapolating the steepest slope of the I-V curve to $V=0$.

The temperature dependence of I_c in zero applied field is well behaved.[18] For temperatures greater than 6.6 K the Josephson penetration depth, λ_J, is larger than the width of the junction, $W/2$, so the current flow through the junction is uniform.[4] In the region from 6.6 to 7.25 K, $I_c^{1/2}$ is linear in temperature as expected.[18] Below 6.6 K the exponential term takes over.[19] Above 7.2 K the coherence distance becomes comparable to the barrier thickness and $I_c^{1/2}$ drops more rapidly than linear in T, as expected.[18]

Vortex trapping

To trap a vortex in the junction, we usually cool the junction through T_c in some fixed perpendicular field, H_z^c, ranging from zero to 50 mOe. For the $W=46$ μm square junction, the first trapped vortex might be expected to occur at $\phi_0/W^2=10$ mOe. It is found experimentally to occur at $+22$ and -16 mOe for the two opposite field directions for the junction reported in detail here.

To conduct the experiment the Fraunhofer pattern is measured for no trapped vortices to confirm good quality of the junction. The $\mathbf{H}=0$ value of I_c, I_{c0}, is measured and used as a prime diagnostic tool. For this junction the value of H_y needed to give one flux quantum is $H_1=0.365$ Oe and I_{c0} is 0.176 mA at 6.9 K. To trap a vortex the sample is cooled through T_c in some field H_z^c and then H_z^c is turned off. The resulting value of I_{c0} is plotted as a function of H_z^c to obtain the step pattern shown in Fig. 1. These data are completely reproducible as long as the sample is not warmed above liquid-nitrogen temperature where the junction anneals. The junctions were kept below 20 K for periods of several months while the research was in progress. The steps are not symmetric about H_z^c, even allowing for a small zero-field offset due to incomplete cancellation of the ambient field by the mu-metal shields. The step labeled 1^+ is much longer than 1^-. The suppression of I_c at the step 2^+ is not the same as at 2^-. In fact the step 3^- has an I_c larger than 2^-, whereas the step 3^+ is smaller than 2^-. This means that the pinning potentials depend somewhat on the magnetic-field direction. The fact that step 3^- has I_c larger than the step 2^- simply means that there are two or more vortices in the junction and some of the fields cancel rather than adding.

Locating vortices

To find the location of the vortex of step 1^+, complete diffraction patterns, I_c versus H_y and I_c versus H_z, are taken and fit to the model,[1] where all image vortices[10] are taken into account. The best fit is found for a vortex that threads both the primary and the secondary layers with very little misalignment. The location in the primary is $(x=0.12,\ y=0.27)$ and the vortex in the secondary is at (0.06,0.19) in units of $W/2$. Details of this fit are presented elsewhere.[1,10]

The quality of the fits and the accuracy in determining the location of the vortex are typified by the diffraction patterns for step 2^+ and 2^- shown in Fig. 2. For these steps, it is found that good fits are obtained for a vortex

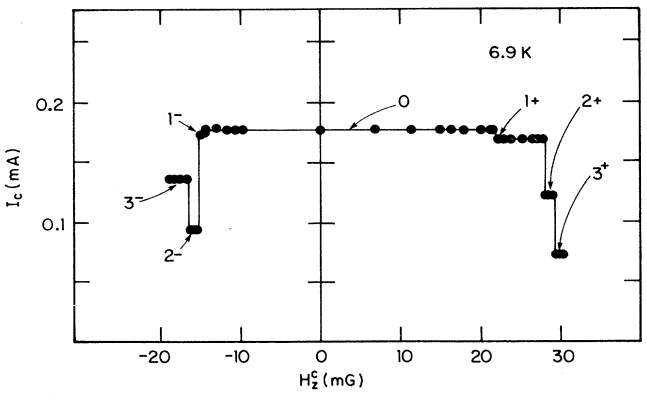

FIG. 1. Step pattern for the zero-field critical current as successive vortices are trapped in the junction.

that threads the primary and leaks out the edge of the junction (we call this a monopole) rather than threading through both the primary and secondary (a dipole). For step 2^+, we first tried to fit the data with just one vortex and a reasonably good fit is found for a monopole at $(0.59,-0.20)$. As shown in Fig. 2(a), the fit of I_c/I_{c0} versus H_y/H_1 is good near the central maximum but the minima in the model (solid line) do not come at the same places as the data (open circles). Using the location of this best fit for H_y, one can also compare the model and data for I_c/I_{c0} versus H_z/H_1 shown in Fig. 2(b). Note that the central peak is not quite right, and the fit near $H_z/H_1=-1$ is poor.

The situation can be greatly improved if one retains the slightly misaligned dipole of step 1^+ at the same location $[+(0.12,0.27)$ and $-(0.06,0.19)$, where $+$ $(-)$ followed by coordinates denotes $N(S)$ pole] and add a monopole whose location is adjustable. In this case, the best fit for the monopole is $+(0.57,-0.14)$, as shown in Figs. 2(c) and 2(d). Note that the minima now come at the correct field values and I_c/I_{c0} versus H_z/H_1 gives a much better fit. In fact, for all steps we find the best fit for the original dipole at the same position near the center of the junction plus a monopole at some other location.

The reason that the junction always traps a dipole near the center is not really understood, but we suspect that it arises from the character of Meissner current patterns. When the junction is cooled through T_c, Meissner currents are established around the outside of the film. As the coherence distance shrinks from infinity to its low-temperature value it leaves a free-energy minimum for the vortex core at the center of the junction. For the second and third vortices the free energy minimum is controlled by dislocations or other sample defects.

Similar plots for the step 2^- are shown in Fig. 3. For this step, the pattern is much more distorted. With one adjustable monopole (S pole) there is a reasonable fit at $(0.43,-0.07)$ as shown in Figs. 3(a) and 3(b). The fit is much improved by adding the dipole of the step 1^+. In this case, the monopole (S pole) is found at $(0.42,-0.09)$.

Using these techniques the vortex location can be determined to about 1% of W or about ± 0.5 μm for this junction. The precision should scale with W because it is the fractional part of a flux quantum which controls the changes in the diffraction pattern.

Vortex motion

To observe the motion of the vortex, the junction might, for example, be prepared by field cooling in step 2^-. Diffraction patterns are then taken to verify the initial vortex arrangement. Let $I_c(0)$ denote the value of I_c at some specified temperature, say 6.9 K, for step 2^- at $\mathbf{H}=0$. The value of $I_c(0)$ is then measured after applications and removal of I_p at successively higher values, and a plot is made of $I_c(0)$ versus I_p^d, as shown by the solid circles of Fig. 4. Note that there is an abrupt increase in I_c at certain depinning values $I_p=+11$, $+19$, and $+22$ mA. For each plateau full diffraction patterns show that

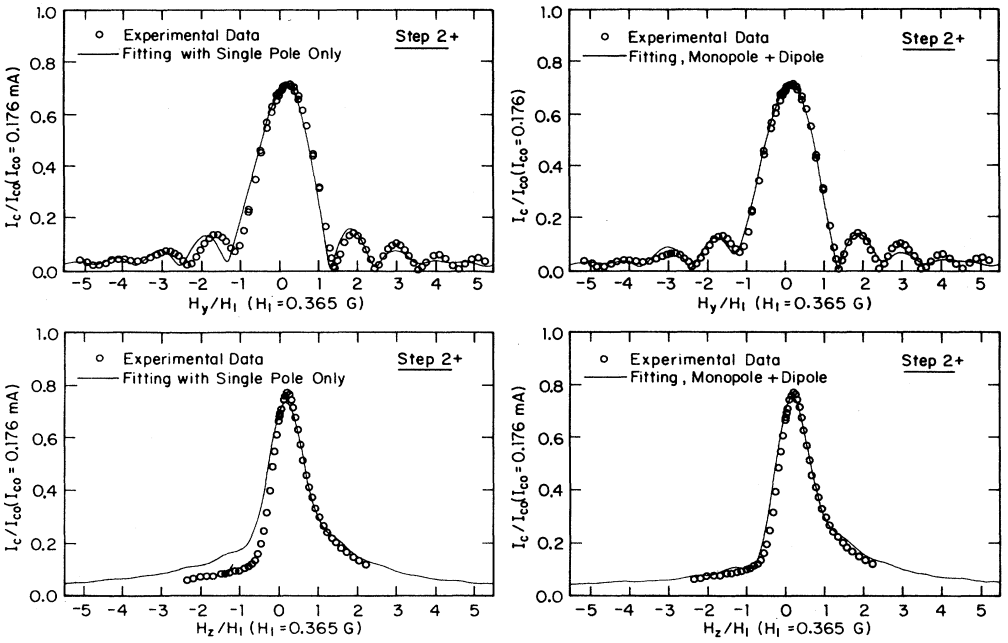

FIG. 2. Fit of the model (solid line) to the data (open circles) for the step 2^+.

the monopole has moved toward the edge of the film. At $+11$ mA the single vortex jumps from the pinning center A to the pinning center B, as shown in Fig. 4. At $+19$ mA it moves from B to C and so forth. At $I_p^d=25$ mA the monopole vortex leaves the junction, and the diffraction patterns, I_c versus H_y and H_z, become those of the step 1^- (or those of the step 1^+ with opposite field direction). This means that the dipole remains near the center of the junction after the monopole has been swept out. At $I_p=38$ mA, a different vortex is nucleated at the edge of the junction and begins to move toward the center. If the direction of I_p is reversed, the monopole moves toward the center of the junction in the two discrete steps, A to G and G to H of Fig. 4. As shown in

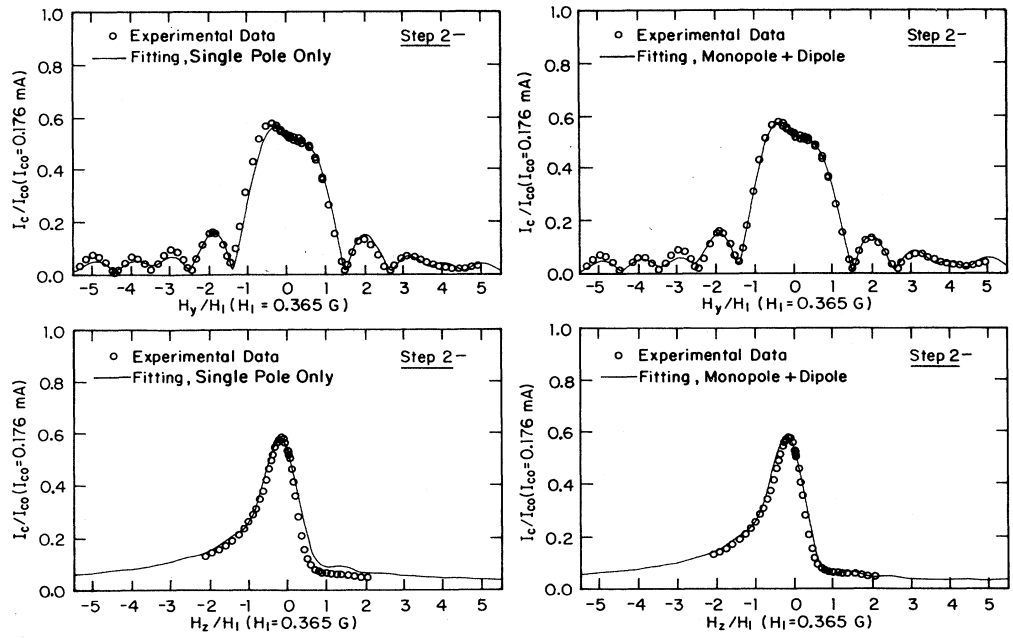

FIG. 3. Fit of the model (solid line) to the data (open circles) for the step 2^-.

Fig. 5, the diffraction patterns for steps E, G, and H show that the vortex motion really causes large changes in the diffraction patterns so the motion is easily resolved. The location of the vortices for each plateau is given in Table I.

To summarize, we find that a force along the x axis causes the vortex to move back and forth along a line nearly parallel to the x axis. There are a number of pinning centers where the vortex stops. The locations where the vortex stops is found to be very reproducible as long as the junction stays below 20 K. If the sample is warmed from 6.9 to 7.0 K, the pinning behavior is similar, except that there are fewer stable pinning sites. If the sample is cooled to 6.8 K, the pinning behavior is again similar, except that there are more stable pinning centers. Upon reversal of I_p, the depinning current value at site A is only 12 mA when pushing toward the edge of the junction but is 22 mA when pushing toward the center. This anisotropy is observed for most pinning sites and shows that the pinning potential is quite asymmetric.

Elementary pinning force

To obtain the elementary pinning force, f_p, from I_p^d, note that $\mathbf{f}_p = \mathbf{j} \times (\phi_0/c)$. Inserting 12 mA for the step A and B of Fig. 4 gives $f_p(A \rightarrow B) = 2.7 \times 10^{-8}$ dyn or an average per unit length of 4.5×10^{-4} dyn/cm. In measurements of the temperature dependence of f_p, pushing the vortex toward the center of the junction and toward the edge of the junction both give $I_p^d \sim (1 - T/T_c)^{3/2}$ over an interval from 6.7 to 7.0 K as reported earlier.[1]

Nucleation at the edge

A problem in measuring f_p for these junctions is that the current used to move the vortex also creates a self field which can nucleate a new vortex at the edge of the junction. The current necessary to nucleate a vortex, I_p^n, has been plotted on Fig. 6 along with the depinning current I_p^d. There is a plateau in I_p^n versus T at $I_p^n \sim 40$

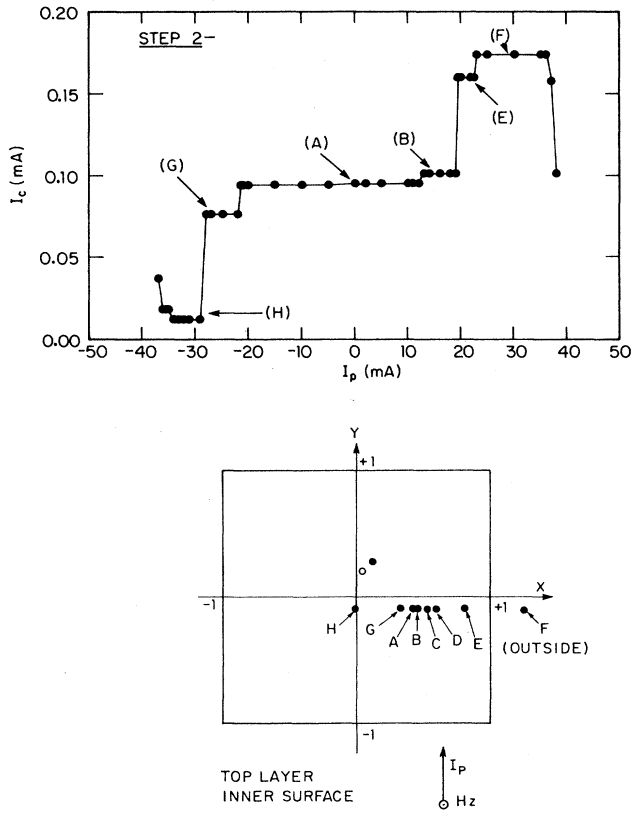

FIG. 4. Changes in the zero-field critical current ($\mathbf{H}=0$) (top) and trajectory of the vortex (bottom) across the junction as the vortex moves across the junction. The single vortex is initially trapped at the pinnning site A.

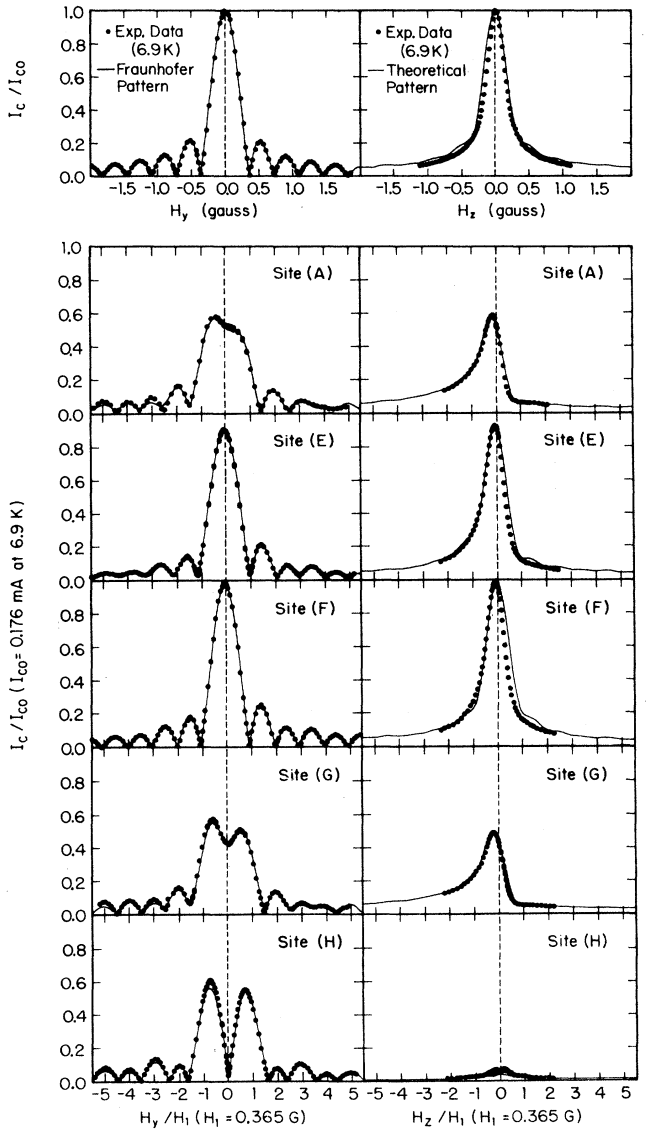

FIG. 5. Diffraction pattern changes (solid circles) and theoretical fits (solid lines) as the vortex moves as shown in the Fig. 4.

TABLE I. Signs preceding parentheses: vortex type. +(−) stands for N pole (S pole). All coordinates are in units of $W/2$.

	Vortex locations		
	Monopole	Dipole	
Step	Primary	Primary	Secondary
1^+		+(0.12,0.27)	−(0.06,0.19)
2^+	+(0.59, −0.14)	+(0.12,0.27)	−(0.06,0.19)
1^-		−(0.12,0.27)	+(0.06,0.19)
2^-A	−(0.42, −0.09)	−(0.12,0.27)	+(0.06,0.19)
2^-B	−(0.44, −0.09)	−(0.12,0.27)	+(0.06,0.19)
2^-C	−(0.53, −0.09)	−(0.12,0.27)	+(0.06,0.19)
2^-D	−(0.59, −0.09)	−(0.12,0.27)	+(0.06,0.19)
2^-E	−(0.81, −0.09)	−(0.12,0.27)	+(0.06,0.19)
2^-F		−(0.12,0.27)	+(0.06,0.19)
2^-G	−(0.33, −0.09)	−(0.12,0.27)	+(0.06,0.19)
2^-H	−(−0.02, −0.10)	−(0.12,0.27)	+(0.06,0.19)

mA. This figure amply illustrates the presence of a small window close to T_c, where $I_p^d < I_p^n$ above 6.7 K and vortex depinning is possible without nucleation.

Flux shuttle

It should be possible to construct a memory or logic device based on the motion of an isolated quantum of flux in a thin film. To build such a device, a single vortex is trapped in one of the S layers; a current in the leg of the junction (I_p) is used to move the vortex or to perform a write operation; a voltage across the Josephson barrier at a fixed bias current is used to determine the location of the vortex or to perform a read operation. Indeed the read operation could be easily performed by biasing the Josephson current to say 0.18 mA and reading off the voltage developed ranging from 0.1 to 1.5 nV for the junction reported here as shown in Fig. 7. A dozen different locations could be determined in the junction and one could conceive a logic with some base other than two if desired.

CONCLUSIONS

It is possible to trap a single vortex in the S layer of a cross-strip Josephson junction and systematically move the vortex back and forth from the center to the edge. Distortions of the diffraction pattern provide an effective tool to locate the vortex, and the position is determined to an accuracy of 1% of the width of the junction or ±500 nm for this example. Over much of the temperature range the flux pinning could not be measured for the strong pinning material Pb-Bi because new vortices would nucleate at the edge of the film before the trapped vortex would move. There is, however, a window about 0.6 K wide near T_c where effective pinning studies can be made. The elementary pinning force was found to vary approximately as $f_p \sim (1-T/T_c)^{3/2}$. The pinning potentials were rather asymmetric with the depinning force along the x axis differing by 50% to 100% depending on the sign of the force.

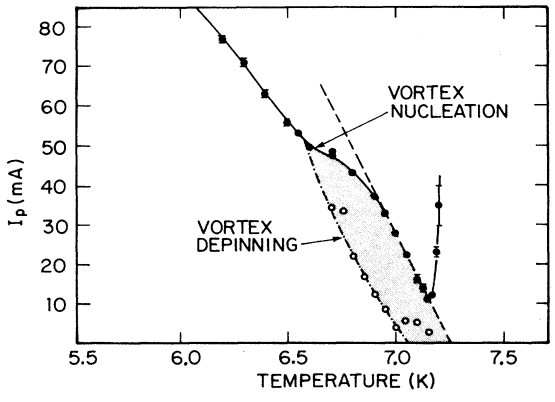

FIG. 6. Temperature dependence of the vortex nucleation current (I_p^n) and depinning current (I_p^d). There is a window close to T_c where $I_p^d < I_p^n$.

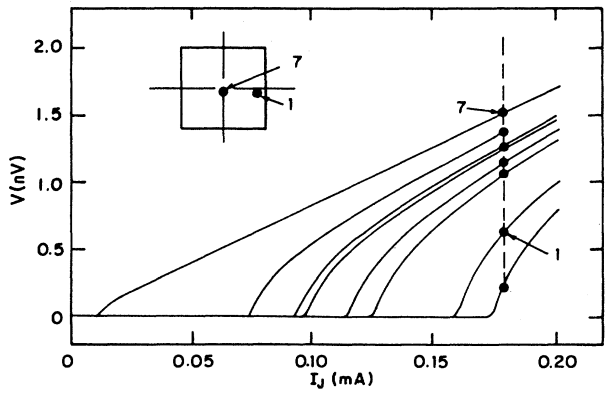

FIG. 7. I-V curve for the junction with a vortex trapped in different places along. Curves are for locations A-H for Fig. 5.

ACKNOWLEDGMENTS

The authors thank J. E. Ostenson and L. Schwartzkopf for technical assistance. Ames Laboratory is operated for the U.S. Department of Energy by Iowa State University under Contract No. W-7405-Eng-82. This work was supported by the Director of Energy Research, Office of Basic Energy Sciences, U.S. Department of Energy.

[1]O. B. Hyun, D. K. Finnemore, L. Schwartzkopf, and J. R. Clem, Phys. Rev. Lett. **58**, 599 (1987).

[2]O. B. Hyun, J. R. Clem, and D. K. Finnemore, in *Proceedings of the International Symposium on Flux Pinning and Electromagnetic Properties of Superconductors, Fukuoka, Japan, 1985,* edited by T. Matsushita, K. Yamafuji, and F. Irie (Matsukuma, Fukuoka, 1985), p. 88.

[3]S. L. Miller, K. R. Biagi, J. R. Clem, and D. K. Finnemore, Phys. Rev. B **31**, 2684 (1985).

[4]A. Barone and G. Paterno, *Physics and Applications of the Josephson Effect* (Wiley, New York, 1982), p. 69.

[5]M. M. Fang, J. R. Clem, and D. K. Finnemore, IEEE Trans. Magn. **MAG-23**, 1196 (1987).

[6]M. Scheuermann, L. R. Lhota, P. K. Kuo, and J. T. Chen, Phys. Rev. Lett. **50**, 74 (1983).

[7]J. J. Chang and D. J. Scalapino, Phys. Rev. B **29**, 2843 (1984).

[8]P. W. Epperlein, H. Seifert, and R. P. Huebener, Phys. Lett. **92A**, 146 (1982).

[9]H. Seifert, R. P. Huebener, and P. W. Epperlein, Phys. Lett. **97A**, 42 (1983); J. R. Clem and R. P. Huebener, J. Appl. Phys. **51**, 2764 (1980).

[10]O. B. Hyun, Ph.D. dissertation, Iowa State University, 1987.

[11]T. A. Fulton, A. F. Hebard, L. N. Dunkelberger, and R. H. Eick, Solid State Commun. **22**, 493 (1977).

[12]A. F. Hebard and R. H. Eick, J. Appl. Phys. **49**, 338 (1978).

[13]J. R. Clem, Phys. Rev. B **9**, 898 (1974).

[14]J. W. Ekin, B. Serin, and J. R. Clem, Phys. Rev. B **9**, 912 (1974).

[15]J. R. Clem, Phys. Rev. B **12**, 1742 (1975).

[16]J. W. Ekin and J. R. Clem, Phys. Rev. B **12**, 1753 (1975).

[17]T. Y. Hsiang and J. Clarke, Phys. Rev. B **21**, 945 (1980); T. Y. Hsiang, *ibid.* **21**, 956 (1980).

[18]J. Clarke, Proc. R. Soc. London, Ser. A **308**, 447 (1969).

[19]T. Y. Hsiang and D. K. Finnemore, Phys. Rev. B **23**, 154 (1980).